Title

Basic fibroblast growth factor uniquely stimulates quiescent vascular smooth muscle cells and induces proliferation and dedifferentiation

Kiyomi Tsuji-Tamura* **and Masato Tamura**

Oral Biochemistry and Molecular Biology, Department of Oral Health Science, Faculty of Dental Medicine and Graduate School of Dental Medicine, Hokkaido University, Kita 13, Nishi 7, Kita-ku, Sapporo 060-8586, Japan

*Author for correspondence: Kiyomi Tsuji-Tamura

Mailing address: Oral Biochemistry and Molecular Biology, Department of Oral Health Science, Faculty of Dental Medicine and Graduate School of Dental Medicine, Hokkaido University, Kita 13, Nishi 7, Kita-ku, Sapporo 060-8586, Japan

E-mail: ktamuratsuji@den.hokudai.ac.jp

Tel: +81-11-706-4243

Keywords

Cell quiescence; vascular smooth muscle cells; vascular endothelial cells; bFGF; TGFβ1; TAGLN

Abbreviations

SMCs: Vascular smooth muscle cells

ECs: Vascular endothelial cells

BMP4: Bone morphogenetic protein 4

CXCL12: Chemokine (C-X-C motif) ligand 12

EPO: Erythropoietin

FGFa: Fibroblast growth factor acidic

bFGF: Basic fibroblast growth factor

IGF-II: Insulin-like growth factor-II

IL-3: Interleukin-3

PDGF-BB: Platelet derived growth factor-BB

SCF: Stem cell factor

SHH: Sonic hedgehog

TGFβ1: Transforming growth factor beta 1

VEGF: Vascular endothelial growth factor 165

WNT-3A: Wingless-type MMTV integration site family, member-3A

TAGLN: Transgelin

Fgfr1: FGF receptor 1

B2m: β-2 microglobulin

Gapdh: glyceraldehyde-3-phosphate dehydrogenase

Srf: serum response factor

Klf4: Kruppel-like factor 4

Abstract

Blood vessels normally remain stable over the long-term. However, in atherosclerosis, vascular cells leave quiescent state and enter activated state. Here, we investigated the factors that trigger breakage of quiescent state by screening growth factors and cytokines using a vascular smooth muscle cell (SMC) line and an endothelial cell (EC) line. Despite known functions of the tested factors, only basic fibroblast growth factor (bFGF) was identified as a potent trigger of quiescence breakage in SMCs, but not ECs. bFGF disrupted tight SMC-monolayers, and caused morphological changes, proliferation and dedifferentiation. Human primary SMCs, but not ECs, also showed similar results. Aberrant SMC-proliferation is a critical event in atherosclerosis. We thus provide further insights into the role of bFGF in vascular pathobiology.

57

58 **Introduction**

59 Vascular blood vessels are lined with a single layer of ECs and surrounded by layers of SMCs (for a
60 review, see [1]). In healthy adult tissues, SMCs and ECs are stable and have a long lifespan. The half-
61 life of SMCs isolated from the mouse aorta ranged from 270 to 400 days [2]. The turnover time of ECs
62 obtained from mouse normal tissues ranged from 47 to 23,000 days [3]. Nevertheless, following
63 chronic exposure of vessels to cardiovascular stress (e.g., dyslipidemia, hyperglycemia, or
64 hypertension), vascular cells leave the quiescent state and become active (for reviews see [4] [5] [6]
65 [7]). Aberrant EC activity occurs, and the release of various factors leads to further cell activation. The
66 proliferation of dedifferentiated SMCs and lipid deposits thicken the intima of arteries. The vessels
67 become narrow and hard, and eventually dysfunctional. This condition is termed atherosclerosis, and
68 can lead to heart attack, heart failure, or stroke. Therefore, the vascular cell transition plays an
69 important role in the initiation of atherosclerosis.

70

71 Cells have unique properties in the quiescent or proliferative state. Confluence and/or serum-deprived
72 culture induced growth arrest and cellular quiescence, and caused distinct changes in gene expression
73 in the mouse fetal fibroblast C3H10T1/2 cell line [8]. Expression of growth factor receptors was low
74 in rabbit aortic SMCs, which formed a confluent layer within a short period [9]. bFGF-induced
75 migration activities increased in rat aortic SMCs cultured after confluence, compared to those of
76 SMCs maintained in the logarithmic phase [10]. Rabbit thoracic aortic SMCs in confluent cultures
77 treated with bFGF showed increased expression of the VEGF gene in a time–dependent manner [11].
78 Sub-confluent and confluent human umbilical vein endothelial cells (HUVECs) showed cell density–
79 dependent expression of numerous genes [12]. Therefore, it is necessary to investigate the effects of
80 factors in the quiescent phase in addition to the growth phase.

81

82 Despite the availability of many studies on vascular cells (for a review, see [1]), the precise molecular
83 cues involved in the switching from an inactive quiescent state to an active proliferative state are still
84 unknown. *In vitro* studies under identical conditions are suitable for the validation of factors in the two

85 types of vascular cells. However, in most protocols, cells are maintained under varied culture
86 conditions, including different specific media, serum and growth factor supplementation, and
87 extracellular matrix. Serum deprivation is useful in the induction of the quiescent state and for the
88 examination of molecular signaling; however, this condition is not tolerated by many *in vitro* models.
89 Therefore, the aim of this study is to identify a trigger factor that breaks the quiescence of vascular
90 cells by comparing the SMC and EC lines, which are maintained under the same conditions and can
91 adapt to serum deprivation.
92
93
94 **Materials and Methods**
95
96 **Cell cultures**
97 The mouse aorta SMC line MOVAS (#CRL-2797, American Type Culture Collection, Manassas, VA,
98 USA), mouse EC line UV♀2 (UV2) (#RCB1994, RIKEN BioResource Research Center, Tsukuba,
99 Japan) and mouse melanoma cell line B16 (#RCB1283, RIKEN BioResource Research Center) were
100 maintained in Dulbecco's Modified Eagle's Medium (Invitrogen, Grand Island, NY, USA) containing
101 10% fetal bovine serum (FBS) (growth medium).
102
103 Human aortic smooth muscle cells (AoSMCs) (#CC-2571, Lonza, MD USA) were cultured in Smooth
104 Muscle Cell Growth Medium 2 (#C-22062, Takara Bio Inc., Shiga, Japan). HUVECs (Human
105 umbilical vein endothelial cells) (#C2519A; Lonza) were cultured in Endothelial Cell Growth Medium
106 Kit (#C-22110; Takara Bio Inc.) on gelatin-coated plates. AoSMCs and HUVECs from passage 3 to 7
107 were used for studies.
108
109 **Antibodies and factors**
110 The mouse monoclonal antibody against β–catenin (#SAB4200720, Sigma–Aldrich, St. Louis, MO,
111 USA, 1:1000), the rabbit polyclonal against transgelin (TAGLN) (#ab14106, Abcam, Cambridge, UK,

112 1:1000) and Phalloidin-iFluor 488 Reagent (#ab176753, Abcam, 1:1000) were used. Although the
113 anti-TAGLN antibody may recognize other TAGLN isoforms [13], it is referred to as TAGLN
114 antibody in this article as shown in the datasheet. Alexa Fluor 546- (#A-11035) and Alexa Fluor 647-
115 (#A32728) conjugated secondary antibodies (Invitrogen, Carlsbad, CA, USA) were used.
116 Recombinant mouse (rm) chemokine (C-X-C motif) ligand 12 (CXCL12, also shown as SDF-1a)
117 (BioLegend, San Diego, CA, USA) and recombinant human (rh) platelet derived growth factor
118 (PDGF)-BB (Austral Biologicals, San Ramon, CA, USA) were used. Rh erythropoietin (EPO) was
119 obtained from Kyowa Hakko Kirin (Tokyo, Japan). Rh FGF acidic (FGFa also known as FGF1), rm
120 bFGF (also known as FGF2), rm sonic hedgehog (SHH), and rm wingless-type MMTV integration site
121 family, member-3A (WNT-3A) were obtained from Novus Biologicals (Littleton, CO, USA).
122 Recombinant human/mouse/rat ACTIVIN-A, rm bone morphogenetic protein 4 (BMP4), rm insulin-
123 like growth factor-II (IGF-II) and rh transforming growth factor β1 (TGFβ1) were obtained from R&D
124 Systems (Minneapolis, MN, USA). Rm interleukin-3 (IL-3), rm stem cell factor (SCF), and rm
125 vascular endothelial growth factor 165 (VEGF) were purchased from PeproTech (Rocky Hill, NJ,
126 USA).
127
128 **Screening for quiescence breakage**
129 Cells were cultured in each growth medium until confluence; the medium was replaced with Human
130 Endothelial-Serum Free Medium (Gibco, Grand Island, NY, USA) (serum-free medium) with a tested
131 factor (refer to text field). For human primary cells, Human Endothelial-Serum Free Medium (Gibco)
132 with 0.1% FBS (low serum medium) was used to induce quiescence. After three days of culture,
133 images of the monolayer of MOVAS and UV2 cells were captured using the live-cell imaging
134 microscopy system IncuCyto Zoom (Essen BioScience, Ann Arbor, MI, USA). For human primary
135 cells, microscope ECLIPSE TS100 (Nikon, Tokyo, Japan) was used to capture images. For a clear
136 observation of the cell morphology, adjustments of brightness and contrast were uniformly applied to
137 the original image using the ImageJ software version 1.440 (National Institutes of Health [NIH],
138 Bethesda, MD, USA). The cell numbers were manually counted.
139

140 **Fluorescent staining and analysis**

141 Cells were fixed in 2% paraformaldehyde in phosphate-buffered saline (PBS) for 15 min at 37 °C.
142 After washing in PBS, the fixed cells were incubated with a blocking buffer containing 0.1% Triton X-
143 100 and 2% skim milk in PBS for 2 h at room temperature; this was followed by incubation with the
144 aforementioned primary antibodies in a blocking buffer overnight at 4 °C. After washing in blocking
145 buffer, the cells were incubated with fluorescent-labeled secondary antibodies for 2 h at room
146 temperature. 4',6-diamidino-2-phenylindole (DAPI, Sigma–Aldrich) was used for the counterstaining
147 of nuclei. Fluorescence images were captured using the FV1000D confocal laser scanning microscope
148 and imaging software (Olympus, Tokyo, Japan). For a clear observation of the cell morphology,
149 adjustments of brightness and contrast were uniformly applied to the original image. Imaging data
150 were analyzed using the ImageJ software (NIH). Cell size and cell-free area were measured through
151 manual tracing. Cell number was determined according to the number of DAPI-stained nuclei in each
152 image. Co-localization area of TAGLN and actin was calculated based on the value of "the merged
153 area of TAGLN and actin"/ "total actin area" in each image.

154

155 **Luciferase reporter assay**

156 The *Tagln* promoter [14] was amplified from the mouse genome by polymerase chain reaction (PCR)
157 using the following primers: forward 5'-<u>GCTCGCTAGCCTCGA</u> AGTCAAGACTAGTTCCCACC-
158 3' and reverse 5'-<u>AGGCCAGATCTTGAT</u>GGGGCGCCGGCTGGGTGAGG-3' (the In-Fusion sites
159 are underlined). The PCR product was inserted into the multi-cloning site of a pGL4.15 firefly
160 luciferase reporter vector (Promega, Madison, WI, USA) using the In-Fusion HD Cloning Kit (Takara
161 Bio Inc.). A pGL4.15 plasmid was co-transfected with pRL-SV40 (Promega) into MOVAS or UV2
162 cells using Xfect mESC Transfection Reagent (Clontech, Palo Alto, CA, USA) according to the
163 instructions provided by the manufacturer. Following transfection, the cells were incubated in serum-
164 free medium for two days and prepared using the Dual-Luciferase Reporter Assay System (Promega).
165 Luciferase activity was measured using the GloMax-Multi Luminescence System (Promega).

166

167 **Quantitative real-time PCR**

168 Total RNA was extracted from the cells using the RNeasy Plus Mini kit (Qiagen, Venlo, Netherlands)
169 and subjected to reverse transcription using the Omniscript Reverse Transcription kit (Qiagen). The
170 relative quantification of gene expression was performed using QuantiTect SYBR Green PCR kits
171 (Qiagen) or Thunderbird Probe qPCR Mix (TOYOBO, Osaka, Japan) in the StepOne real time PCR
172 system (ABI, Foster City, CA, USA). The primer sequences for mouse FGF receptor 1 (*Fgfr1*) were:
173 forward 5'-AGCAGTTGGTGGAAGACCTG-3', reverse 5'-GTACTGGTCCAGCGGTATGG-3'; and
174 for mouse β-2 microglobulin (*B2m*): forward 5'-CTGACCGGCCTGTATGCTAT-3', reverse 5'-
175 CCGTTCTTCAGCATTTGGAT-3'. The probe and primer sequences used for mouse *Tagln* were:
176 probe 5'-AAGAGGGACTTCACAGACAGCCAACTGC-3', forward 5'-
177 ATCCCAACTGGTTTATGAAGdAAAGC-3', reverse 5'-AAGGCCAATGACGTGCTTCC-3';
178 Kruppel-like factor 4 (*Klf4*): probe 5'-ACCAAGAGTTCTCATCTCAAGGCACACCTG-3', forward
179 5'-ACTTGTGACTATGCAGGCTGTG-3', reverse 5'-GGTTTCTCGCCTGTGTGAGTT-3'; mouse
180 *B2m*: probe 5'-ACCGGCCTGTATGCTATCCAGAAAACCC-3', forward 5'-
181 GGTCTTTCTGGTGCTTGTCTCA-3', reverse 5'-GTTCGGCTTCCCATTCTCCG-3'. Predesigned
182 primer and probe sets (TaqMan Gene Expression Assays; ABI) were used for the detection of mouse
183 serum response factor (*Srf*) or mouse glyceraldehyde-3-phosphate dehydrogenase (*Gapdh*) gene. The
184 primer sequences for human *TAGLN* were: forward 5'-GCAAAGACATGGCAGCAGT-3', reverse
185 5'-GCTGGCTCTCTGTGAATTCC-3'; human *SRF*: forward 5'-ATCTGGGACAGTGCAGATCC-3',
186 reverse 5'-CACCTGTAGCTCGGTGAGGT-3'; human *KLF4*: forward 5'-
187 GTTCCCATCTCAAGGCACAC-3', reverse 5'-CCCCGTGTGTTTACGGTAGT-3', and human β–
188 *ACTIN*: forward 5'-AGAGCTACGAGCTGCCTGAC-3', reverse 5'-
189 AGCACTGTGTTGGCGTACAG-3'. The relative levels of gene expression were determined through
190 normalization to the levels of an endogenous control: the expression of *B2m*, *Gapdh* or β–*ACTIN* was
191 quantified by comparison with the control.
192

193 **Statistical analysis**

194 The data are shown as the mean ± standard deviation (s.d.). F-tests followed by two-tailed Student's *t*-
195 tests were used to analyze the results of two groups. For comparison of multiple groups, Tukey's test

196 was performed using MEPHAS (http://www.gen-info.osaka-u.ac.jp/testdocs/tomocom/dunnett-
197 e.html). The p-values < 0.05 denoted statistically significant differences.
198
199
200 **Results**
201
202 **bFGF broke the quiescence of SMCs but not ECs**
203 Contact inhibition, in which growth arrest is obtained by cell–cell contact, and serum deprivation lead
204 to quiescence in non-cancerous cells [8]. To investigate the factors which trigger the disruption of the
205 stable sheet-like appearance of a vascular cell monolayer (referred to as "quiescence breakage" in this
206 report), we performed serum-free confluent culture of the mouse SMC line MOVAS cells and the
207 mouse EC line UV2 cells. Confluent cell layers were treated with ACTIVIN A (20 ng/ml), BMP4 (100
208 ng/ml), CXCL12 (20 ng/ml), EPO (2 U/ml), FGFa (10 ng/ml), bFGF (20 ng/ml), IGF-II (100 ng/ml),
209 IL-3 (20 ng/ml), PDGF-BB(10 ng/ml), SCF (100 ng/ml), SHH (20 ng/ml), TGFβ1 (10 ng/ml), VEGF
210 (20 ng/ml) or WNT-3A (20 ng/ml) in serum-free medium for three days. Microscope images showed
211 tight sheet-like monolayers of flat polygonal-shaped MOVAS cells and epithelial-like–shaped UV2
212 cells in the untreated controls (Fig. 1A). Despite known effects of the tested factors on vascular cells
213 (Table 1, 2), most factors did not affect the quiescent MOVAS and UV2 monolayers (Fig. 1). Only
214 bFGF disrupted the quiescent appearance in the MOVAS monolayer, leading to changes in the
215 morphology (i.e., small spindle shapes) and the new formation of a cell-free area (Fig. 1). However,
216 the bFGF had no effect on the quiescent UV2 monolayer.
217
218 Immunofluorescent staining of β-catenin, a component of adherens junctions, was employed to
219 examine the details of cell morphology. Treatment with bFGF caused a morphological change in
220 MOVAS cells (Fig. 2A), namely a decrease in cell size compared with Control and TGFβ1 (Fig. 2B).
221 The cell-free areas on the culture surfaces were newly spread in MOVAS monolayers treated with
222 bFGF compared with Control and TGFβ1 (Fig. 2C). Moreover, the cell number was increased by
223 bFGF compared with Control and TGFβ1 (Fig. 2D).

224

225 In UV2, there were no significant differences observed between the Control, bFGF, and TGFβ1
226 groups in cell size (Fig. 2A, B), cell-free area (Fig. 2C), and cell number (Fig. 2D). These results
227 suggest that bFGF broke the established cell quiescence in a cell type–specific manner.

228

229 **bFGF-induced smooth muscle change, which was accompanied by reduction of TAGLN**

230 The actin-bundling protein TAGLN is abundantly expressed in differentiated SMCs [15], and
231 recognized as one of the myogenic differentiation markers. Differentiated SMCs have a quiescent
232 contractile phenotype with low proliferation rate and high levels of myogenic markers (for a review,
233 see [16]). When SMCs undergo dedifferentiation, they show a change in cell shape, a high
234 proliferation rate and low expression of myogenic markers, resulting in an active synthetic phenotype.
235 TAGLN expression is suppressed during the process of dedifferentiation (for a review, see [16]). In
236 the control MOVAS cells, TAGLN was co-localized with filamentous actin in the polygonal
237 cytoplasm (Fig.3A). bFGF caused strong accumulation of actin at the margins (Fig. 3A) and decreased
238 the co-localization of TAGLN compared with Control and TGFβ1 (Fig. 3B). TGFβ1 induced
239 prominent filamentous actin (Fig. 3A), and the co-localization of TAGLN with actin was similar to
240 that noted in the controls (Fig. 3B). SMC dedifferentiation is characterized by a transition to a
241 proliferative phenotype with a reduction of SMC markers, including TAGLN (for a review, see [16]).
242 Therefore, these findings imply that bFGF-induced breakage of quiescence results in the proliferative
243 dedifferentiation of SMCs.

244

245 TAGLN expression also has been described in non-SMCs including mesenchymal cells, kidney cell
246 lines or ECs [17] [18] [19][13]. TAGLN was also present in UV2 cells and co-localized with
247 filamentous actin in the cytoplasm in the controls (Fig. 3C). Treatment with bFGF or TGFβ1 did not
248 have a significant effect on the co-localization of TAGLN compared with the controls (Fig. 3D),
249 suggesting that the effect of bFGF on TAGLN distribution may be specific to SMCs.

250

251 **bFGF decreased the expression of *Tagln* and *Srf* genes in SMCs but not ECs**

252 FGF binds to and activates the receptor tyrosine kinase FGFR (for a review, see [20]). The expression
253 of *Fgfr1* (coding for FGFR1, a high affinity receptor for bFGF) was assessed to rule out the possibility
254 that the non-response of the UV2 monolayer to bFGF may be due to the lack of FGFR1. *Fgfr1* was
255 fully and highly expressed in MOVAS and UV2 cells compared with B16 cells (Fig. 4A). These
256 results indicated that bFGF may be specifically involved in the breakage of quiescence of SMCs,
257 regardless of the presence of the receptor. Moreover, consistent with the expression of TAGLN
258 proteins (Fig. 3), the significant transcriptional activity of the *Tagln* promoter was detected in
259 MOVAS and UV2 cells (Fig. 4B). bFGF downregulated the expression of *Tagln* and *Srf* genes in
260 MOVAS cells compared with Control. TGFβ1 upregulated the expression of *Tagln* and *Klf4* genes
261 compared with Control (Fig. 4C). The expression levels of *Tagln*, *Srf*, and *Klf4* genes were not
262 significantly different in UV2 cells treated with Control, bFGF, or TGFβ1 (Fig. 4C). SRF and Klf4 are
263 important transcription factors for SMC differentiation [21] [22]. Therefore, bFGF and TGFβ1
264 regulate the expression of *Srf* and *Klf4*, respectively. Consequently, they may contribute to the
265 transcription of *Tagln* in quiescent SMCs.
266
267 Of note, bFGF and TGFβ1 appear to exert opposite effects on *Tagln* transcription (Fig. 4C).
268 Therefore, we investigated whether the effect of bFGF can be reversed by TGFβ1. Co-treatment with
269 bFGF and TGFβ1 disrupted quiescence in the MOVAS monolayer and caused a similar morphological
270 change to that induced by single treatment with bFGF (Fig. 5). This evidence demonstrated that
271 TGFβ1 failed to prevent the breakage of quiescence induced by bFGF. The features of the UV2
272 monolayer were not affected by bFGF with or without TGFβ1 (Fig. 5).
273
274 **bFGF broke the quiescence of human primary SMCs but not of human primary ECs**
275 We extended our study by using human primary SMCs (AoSMCs) and human primary ECs
276 (HUVECs) to confirm the effects of bFGF. Confluent primary cell layers were treated with bFGF (20
277 ng/ml) or TGFβ1 (10 ng/ml) in low serum medium for three days. In the untreated controls, AoSMCs
278 showed tight sheet-like monolayers of polygonal-shaped cells (Fig. S1). HUVECs showed a dispersed
279 population of endothelial-shaped cells, as some cells could not survive under low serum condition

280 (Fig. S1). bFGF caused most AoSMCs to shift to a small round shape, but some cells remained
281 polygonal. bFGF did not affect the shape of HUVECs. TGFβ1 had no effect on cell shapes in
282 AoSMCs or HUVECs. The β-catenin staining showed that bFGF reduced cell size and increased the
283 number of cells in AoSMCs compared with Control and TGFβ1 (Fig. S2). HUVECs showed no
284 significant alteration of cell size and cell number during treatment with Control, bFGF, or TGFβ1
285 (Fig. S2). TAGLN co-localized with actin in AoSMCs and HUVECs in the untreated controls (Fig.
286 S3). The co-localized area in AoSMCs were decreased by bFGF, and increased by TGFβ1. No
287 significant difference in the co-localization ratio was found in HUVECs in the Control, bFGF, or
288 TGFβ1 groups. The expression of *TAGLN* gene in AoSMCs were decreased by bFGF and increased
289 by TGFβ1, which generally correlate with the expression of SRF and KLF4 genes (Fig. S4A). These
290 gene expression levels were not significantly different in HUVECs in the three groups (Fig. S4B).
291
292 These results with AoSMCs and HUVECs appear to be consistent with the results for MOVAS and
293 UV2 cells. Furthermore, co-treatment of TGFβ1 also did not reverse the effect of bFGF in AoSMCs
294 (Fig. S5). These findings suggest that bFGF may exert a unique effect on SMC lineages in a quiescent
295 state.
296
297
298 **Discussion**
299
300 In this study, we performed screening of factors in serum-free confluent cultures of an SMC line or an
301 EC line to identify potential factors involved in the breakage of vascular cell quiescence. We found
302 that bFGF triggered the disruption of quiescence in the SMC monolayer, but not in the EC monolayer.
303 Treatment with bFGF induced morphological changes and proliferation, accompanied by reduction of
304 the SMC marker. This suggests that bFGF caused SMC-specific breakage of quiescence, almost
305 simultaneously a proliferative dedifferentiation. Similar effects of bFGF were also observed in human
306 primary SMCs and human primary ECs in low serum confluent cultures. Although it has been reported
307 that numerous factors regulate the proliferation or migration of SMCs in varied cellular contexts

308 (Table 1), our screening demonstrated that only bFGF altered quiescent appearance in the SMC
309 monolayer. Therefore, breakage of SMC-quiescence may be a unique process specifically triggered by
310 bFGF.
311
312 bFGF is a member of the family of heparin-binding proteins, and a mitogen for various cell types
313 including SMCs and ECs [23] (for a review, see [24]). Antisense inhibition of endogenous bFGF
314 suppressed DNA synthesis, and induced apoptosis in rat aortic SMCs [25] [26]. bFGF and TGFβ1
315 antagonistically regulate myogenic differentiation. The expression of *Tagln* in 10T1/2 cells, rat aortic
316 SMCs, and human airway SMCs was upregulated by TGFβ1; notably, these effects were neutralized
317 by bFGF [27] [28]. Interference with FGF signaling using *Fgfr1* siRNA increased TGFβ signaling
318 activity in human aortic SMCs cultured for a long period of time in low-serum medium [29]. Our
319 results showed the opposite effect of bFGF and TGFβ on *Tagln* transcription. However, interestingly,
320 the bFGF-induced breakage of quiescence was not inhibited by TGFβ1. The cellular responses to
321 TGFβ have been reported to be influenced by cellular contexts such as cell-type, cell density or the
322 presence of other factors [30] [31]. TGFβ1 promoted mitosis induced by bFGF in confluent rat aortic
323 SMCs [31]. These findings suggest that the responses of SMCs rely on cellular contexts, such as cell
324 density [30].
325
326 The transcription of myogenic genes, including *Tagln*, is regulated by SRF and KLF4 via binding to
327 CArG boxes and TGFβ1 control element sites [32] [33] (for a review, see [34]). SRF and KLF4 act
328 pleiotropically in the presence of bFGF and TGFβ1 [27] [21] [35] [33] [36]. Our results showed that
329 *Tagln* expression corresponded to significant changes in the *Srf* and *Klf4* genes in SMCs stimulated
330 with bFGF and TGFβ1, suggesting a putative transcriptional regulation of *Tagln*.

331 VEGF is an essential factor for endothelial activation. We also have previously shown the role of
332 VEGF in vascular-tube formation *in vitro* [37] [38] [39], and vascular development *in vivo* [40] [41]
333 (for reviews, see [42] [43]). bFGF stimulates proliferation and migration of ECs [44] (for a review, see
334 [45]). TGFβ1 attenuated EC proliferation and promoted tube formation [46]. Despite the known

335 effects of factors (e.g., VEGF, bFGF and TGF1) on ECs (Table 2), our screening did not reveal factors
336 associated with the breakage of quiescence in ECs. Although the FGF receptor was more abundant in
337 ECs than SMCs, bFGF exerted SMC-specific effects. These findings appear to resemble an early
338 histological event of atherosclerosis with proliferation of SMCs, but not ECs. Synergistic effects of
339 CXCL12 and VEGF, or BMP4 and heat shock protein (HSP) 70 have been reported in promotion of
340 proliferation, migration, or tube-formation [47] [48]. Therefore, the breakage of quiescence in the EC
341 monolayer may require other stimuli or multiple factors. Further studies are warranted to investigate
342 the mechanisms involved in this process.

343 *Tagln* has widely accepted to be a canonical marker of SMCs. Therefore, ECs expressing *Tagln* are
344 conventionally recognized as undergoing endothelial-to-mesenchymal transition (EndMT). EndMT
345 has been observed in pathological vascular conditions including atherosclerosis (for a review, see [4]).
346 TGFβ has been reported to induce EndMT, which is augmented or attenuated by bFGF in the various
347 contexts. The feature of EndMT *in vitro* is derived under certain stimulation such as a mechanical
348 strain or a prolonged culture, in which ECs express SMC markers and show morphological changes
349 [49] [50]. On the other hand, we recently detected activated transcription of *Tagln* in elongated ECs
350 under angiogenic stimuli [13]. It has been reported that *Tagln* expression is induced following the
351 contact and spreading of mesenchymal cells on an adherent surface [17] [18]; *Tagln* is sensitive to
352 changes in the morphology of non-SMCs. Therefore, the elevated expression of *Tagln* may be related
353 to physiological morphological changes in ECs, in addition to pathological processes such as EndMT.
354 Consistent with this line of thought, the present results showed that ECs with unchanged morphology
355 expressed similar levels of *Tagln* regardless of bFGF and TGFβ1.
356

357 SMCs have multiple and independent developmental origins including mesoderm and neural crest (for
358 a review, see [51], and are well known to exhibit phenotypic heterogeneity in various parameters
359 including cell shape, marker expression, proliferative activity and cellular responses to stimuli [52]
360 (for a review, see [53]). Our study showed that MOVAS cells were highly uniform in shape under
361 bFGF treatment, while AoSMCs had some mixture of the different cell shapes. This may be due to the

property of MOVAS cells as a single-clone cell line and the heterogeneity of the primary cell population of AoSMCs. Although the bFGF-induced morphological change in AoSMCs was not as prominent as in MOVAS cells, it was similarly associated with the proliferation and dedifferentiation. On the other hand, ECs are recognized to arise from the mesoderm, and erythro-myeloid progenitors (EMPs) were recently reported as one of the origins (for a review, see [54]). ECs have a strong heterogeneity depending on organs and within the capillaries of each organ (for a review, see [55]), and HUVECs also do [56]. In the current study, HUVECs appear to contain at least two populations which were sensitive and insensitive to a low serum condition, respectively. The surviving cells were not affected by bFGF and TGFβ1, similar to UV2 cells. Our study suggests that the cell lines may represent a part of the heterogeneous properties in primary cell populations, and serum-free confluent culture of the cell lines may be useful to examine cellular responses in the quiescent state.

In this report, we showed that bFGF caused breakage of quiescence in SMCs and led to proliferative dedifferentiation. These bFGF-induced effects may be cell-type specific and may be a unique response independent of that shared with other factors (Table 1, 2). The phenotypic transition of SMCs is a key component of atherosclerosis. Our results may provide a new insight into bFGF as a potent trigger of dysfunction in SMCs.

Data Availability

The data that support the findings of this study are available from the corresponding author [ktamuratsuji@den.hokudai.ac.jp] upon reasonable request.

Acknowledgements

This work was supported by KAKENHI [grant number: 18K0978208] from the Japan Society for the Promotion of Science (JSPS).

Conflict of Interest Statement

The authors declare that they have no competing interests.

Author Contributions

K. Tsuji-Tamura designed and performed research, and analyzed data. M. Tamura helped perform experiments. All authors wrote the paper.

References

1 Conway EM, Collen D & Carmeliet P (2001) Molecular mechanisms of blood vessel growth. *Cardiovasc Res* **49**, 507–521.

2 Neese RA, Misell LM, Turner S, Chu A, Kim J, Cesar D, Hoh R, Antelo F, Strawford A, Mccune JM, Christiansen M & Hellerstein MK (2002) Measurement in vivo of proliferation rates of slow turnover cells by 2 H 2 O labeling of the deoxyribose moiety of DNA. *Proceedings of the National Academy of Sciences of the United States of America* **99**, 15345–15350.

3 Hobson B & Denekamp J (1984) Endothelial proliferation in tumours and normal tissues: Continuous labelling studies. *Br J Cancer* **49**, 405–413.

4 Low EL, Baker AH & Bradshaw AC (2019) TGFβ smooth muscle cells and coronary artery disease: a review. *Cellular Signalling* **53**, 90–101.

5 Theodorou K & Boon RA (2018) Endothelial cell metabolism in atherosclerosis. *Frontiers in Cell and Developmental Biology* **6**.

412 6 Liekens S, de Clercq E & Neyts J (2001) Angiogenesis: regulators and clinical applications.

413 *Biochemical Pharmacology* **61**, 253–270.

414 7 Muto A, Fitzgerald TN, Pimiento JM, Maloney SP, Teso D, Paszkowiak JJ, Westvik TS, Kudo FA,

415 Nishibe T & Dardik A (2007) Smooth muscle cell signal transduction: Implications of vascular

416 biology for vascular surgeons. *Journal of Vascular Surgery* **45**, 15a–24a.

417 8 Gos M, Miloszewska J, Swoboda P, Trembacz H, Skierski J & Janik P (2005) Cellular quiescence

418 induced by contact inhibition or serum withdrawal in C3H10T1/2 cells. *Cell Proliferation* **38**,

419 107–116.

420 9 Saltis J, Thomasb AC, Agrotis A, Campbellb JH, Campbellb GR, Bobik A & Alfred-Baker " " (1995)

421 Expression of growth factor receptors on arterial smooth muscle cells. Dependency on cell

422 phenotype and serum factors. *Atherosclerosis* **118**, 77–87.

423 10 Wen J-K, Han M, Zheng B & Yang S-L (2002) Comparison of gene expression patterns and

424 migration capability at quiescent and proliferating vascular smooth muscle cells stimulated by

425 cytokines. *Life Sciences* **70**, 799–807.

426 11 Stavri GT, Zachary IC, Baskerville PA, Martin JF & Erusalimsky JD (1995) Basic Fibroblast

427 Growth-Factor up-Regulates the Expression of Vascular Endothelial Growth-Factor in Vascular

428 Smooth-Muscle Cells - Synergistic Interaction with Hypoxia. *Circulation* **92**, 11–14.

429 12 Fontijn RD, Volger OL, Fledderus JO, Reijerkerk A, de Vries HE & Horrevoets AJG (2008) SOX-
430 18 controls endothelial-specific claudin-5 gene expression and barrier function. *Am J Physiol*
431 *Heart Circ Phys-iol* **294**, 891–900.
432 13 Tsuji-Tamura K, Morino-Koga S, Suzuki S & Ogawa M (2021) The canonical smooth muscle cell
433 marker TAGLN is present in endothelial cells and is involved in angiogenesis. *Journal of Cell*
434 *Science* **134**.
435 14 Akyurek LM, Yang ZY, Aoki K, San H, Nabel GJ, Parmacek MS & Nabel EG (2000) SM22alpha
436 promoter targets gene expression to vascular smooth muscle cells in vitro and in vivo. *Mol Med*
437 **6**, 983–991.
438 15 Lees-Miller JP, Heeley DH & Smillie LB (1987) *An abundant and novel protein of 22 kDa (SM22)*
439 *is widely distributed in smooth muscles Purification from bovine aorta*.
440 16 Doevendans PA & van Eys G (2002) Smooth muscle cells on the move: the battle for actin.
441 *Cardiovascular Research* **54**, 499–502.
442 17 Shapland C, Lowings P & Lawson D (1988) Identification of new actin-associated polypeptides
443 that are modified by viral transformation and changes in cell shape. *Journal of Cell Biology* **107**,
444 153–161.
445 18 Shapland C, Hsuan JJ, Totty NE & Lawson D (1993) Purification and Properties of Transgelin: A
446 Transformation and Shape Change Sensitive Actin-gelling Protein. *J Cell Biol* **121**, 1065–1073.

447 19 Chen J, Kitchen CM, Streb JW & Miano JM (2002) Myocardin: A Component of a Molecular
448 Switch for Smooth Muscle Differentiation. *Journal of Molecular and Cellular Cardiology* **34**,
449 1345–1356.
450 20 Eswarakumar VP, Lax I & Schlessinger J (2005) Cellular signaling by fibroblast growth factor
451 receptors. *Cytokine and Growth Factor Reviews* **16**, 139–149.
452 21 Nishida W, Nakamura M, Mori S, Takahashi M, Ohkawa Y, Tadokoro S, Yoshida K, Hiwada K,
453 Hayashi K & Sobue K (2002) A triad of serum response factor and the GATA and NK families
454 governs the transcription of smooth and cardiac muscle genes. *Journal of Biological Chemistry*
455 **277**, 7308–7317.
456 22 Wassmann S, Wassmann K, Jung A, Velten M, Knuefermann P, Petoumenos V, Becher U, Werner
457 C, Mueller C & Nickenig G (2007) Induction of p53 by GKLF is essential for inhibition of
458 proliferation of vascular smooth muscle cells. *Journal of Molecular and Cellular Cardiology* **43**,
459 301–307.
460 23 Davis MG, Zhou M, Ali S, Coffin JD, Doetschman T & Dorn GW (1997) Intracrine and autocrine
461 effects of basic fibroblast growth factor in vascular smooth muscle cells. *Journal of Molecular*
462 *and Cellular Cardiology* **29**, 1061–1072.
463 24 Chung J & Shum-Tim D (2012) Neovascularization in Tissue Engineering. *Cells* **1**, 1246–1260.
464 25 Fox JC & Shanley JR (1996) Antisense inhibition of basic fibroblast growth factor induces
465 apoptosis in vascular smooth muscle cells. *Journal of Biological Chemistry* **271**, 12578–12584.

466 26 Itoh H, Mukoyama M, Pratt RE, Gibbons GH & Dzau VJ (1993) Multiple autocrine growth factors
467 modulate vascular smooth muscle cell growth response to angiotensin II. *Journal of Clinical*
468 *Investigation* **91**, 2268–2274.
469 27 Kawai-Kowase K, Sato H, Oyama Y, Kanai H, Sato M, Doi H & Kurabayashi M (2004) Basic
470 fibroblast growth factor antagonizes transforming growth factor-β1-induced smooth muscle gene
471 expression through extracellular signal-regulated kinase 1/2 signaling pathway activation.
472 *Arteriosclerosis, Thrombosis, and Vascular Biology* **24**, 1384–1390.
473 28 Schuliga M, Javeed A, Harris T, Xia Y, Qin C, Wang Z, Zhang X, Lee PVS, Camoretti-Mercado B
474 & Stewart AG (2013) Transforming growth factor-β-Induced differentiation of airway smooth
475 muscle cells is inhibited by fibroblast growth factor-2. *American Journal of Respiratory Cell and*
476 *Molecular Biology* **48**, 346–353.
477 29 Chen PY, Qin LF, Li GX, Tellides G & Simons M (2016) Fibroblast growth factor (FGF) signaling
478 regulates transforming growth factor beta (TGF beta)-dependent smooth muscle cell phenotype
479 modulation. *Scientific Reports* **6**.
480 30 Majack RA (1987) Beta-Type Transforming Growth Factor Specifies Organizational Behavior in
481 Vascular Smooth Muscle Cell Cultures. *The Journal of Cell Biology* **106**, 465–471.
482 31 Majack RA, Majesky MW & Goodman L v (1990) Role of PDGF-A Expression in the Control of
483 Vascular Smooth Muscle Cell Growth by Transforming Growth Factor. *TheJournalof Cell*
484 *Biology* **111**, 239–247.

485 32 Kim S, Ip HS, Lu MM, Clendenin C & Parmacek MS (1997) A Serum Response Factor-Dependent
486 Transcriptional Regulatory Program Identifies Distinct Smooth Muscle Cell Sublineages.
487 *MOLECULAR AND CELLULAR BIOLOGY* **17**, 2266–2278.
488 33 Adam PJ, Regan CP, Hautmann MB & Owens GK (2000) Positive- and negative-acting Kruppel-
489 like transcription factors bind a transforming growth factor β control element required for
490 expression of the smooth muscle cell differentiation marker SM22α in vivo. *Journal of*
491 *Biological Chemistry* **275**, 37798–37806.
492 34 Kumar MS & Owens GK (2003) Combinatorial control of smooth muscle-specific gene expression.
493 *Arteriosclerosis, Thrombosis, and Vascular Biology* **23**, 737–747.
494 35 Qiu P, Feng XH & Li L (2003) Interaction of Smad3 and SRF-associated complex mediates TGF-
495 β1 signals to regulate SM22 transcription during myofibroblast differentiation. *Journal of*
496 *Molecular and Cellular Cardiology* **35**, 1407–1420.
497 36 Li HX, Han M, Bernier M, Zheng B, Sun SG, Su M, Zhang R, Fu JR & Wen JK (2010) Krüppel-
498 like factor 4 promotes differentiation by transforming growth factor-β receptor-mediated Smad
499 and p38 MAPK signaling in vascular smooth muscle cells. *Journal of Biological Chemistry* **285**,
500 17846–17856.
501 37 Park S-H, Sakamoto H, Tsuji-Tamura K, Furuyama T & Ogawa M (2009) Foxo1 is essential for in
502 vitro vascular formation from embryonic stem cells. *Biochemical and Biophysical Research*
503 *Communications* **390**.

38 Tsuji-Tamura K & Ogawa M (2018) Dual inhibition of mTORC1 and mTORC2 perturbs cytoskeletal organization and impairs endothelial cell elongation. *Biochemical and Biophysical Research Communications* **497**, 326–331.

39 Tsuji-Tamura K & Ogawa M (2016) Inhibition of the PI3K-Akt and mTORC1 signaling pathways promotes the elongation of vascular endothelial cells. *Journal of Cell Science* **129**, 1165–1178.

40 Tsuji-Tamura K, Sato M, Fujita M & Tamura M (2020) Glycine exerts dose-dependent biphasic effects on vascular development of zebrafish embryos. *Biochemical and Biophysical Research Communications* **527**, 539–544.

41 Tsuji-Tamura K, Sato M, Fujita M & Tamura M (2020) The role of PI3K/Akt/mTOR signaling in dose-dependent biphasic effects of glycine on vascular development. *Biochemical and Biophysical Research Communications* **529**, 596–602.

42 Tsuji-Tamura K, Sakamoto H & Ogawa M (2011) ES Cell Differentiation as a Model to Study Cell Biological Regulation of Vascular Development. In *Embryonic Stem Cells: The Hormonal Regulation of Pluripotency and Embryogenesis (ed. C. S. Atwood)* pp. 581–606.

43 Tsuji-Tamura K & Ogawa M (2018) Morphology regulation in vascular endothelial cells. *Inflammation and Regeneration* **38**.

44 Jih YJ, Lien WH, Tsai WC, Yang GW, Li C & Wu LW (2001) Distinct regulation of genes by bFGF and VEGF-A in endothelial cells. *Angiogenesis* **4**, 313–321.

522 45 Lamalice L, le Boeuf F & Huot J (2007) Endothelial cell migration during angiogenesis.
523 *Circulation Research* **100**, 782–794.
524 46 Madri JA, Pratt BM & Tucker AM (1988) Phenotypic Modulation of Endothelial Cells by
525 Transforming Growth Factor-13 Depends upon the Composition and Organization of the
526 Extracellular Matrix. *J Cell Biol* **106**, 1375–1384.
527 47 Kryczek I, Lange A, Mottram P, Alvarez X, Cheng P, Hogan M, Moons L, Wei S, Zou L, Machelon
528 V, Emilie D, Terrassa M, Lackner A, Curiel TJ, Carmeliet P & Zou W (2005) CXCL12 and
529 Vascular Endothelial Growth Factor Synergistically Induce Neoangiogenesis in Human Ovarian
530 Cancers. *Cancer Res* **65**, 465–472.
531 48 Yao Y, Watson AD, Ji S & Boström KI (2009) Heat shock protein 70 enhances vascular bone
532 morphogenetic protein-4 signaling by binding Matrix Gla protein. *Circulation Research* **105**,
533 575–584.
534 49 Cevallos M, Riha GM, Wang X, Yang H, Yan S, Li M, Chai H, Yao Q & Chen C (2006) Cyclic
535 strain induces expression of specific smooth muscle cell markers in human endothelial cells.
536 *Differentiation* **74**, 552–561.
537 50 Frid MG, Kale VA & Stenmark KR (2002) Mature vascular endothelium can give rise to smooth
538 muscle cells via endothelial-mesenchymal transdifferentiation: In vitro analysis. *Circulation*
539 *Research* **90**, 1189–1196.

51 Majesky MW, Dong XR, Regan JN & Hoglund VJ (2011) Vascular smooth muscle progenitor cells: Building and repairing blood vessels. *Circulation Research* **108**, 365–377.

52 Hao H, Ropraz P, Verin V, Camenzind E, Geinoz A, Pepper MS, Gabbiani G & Bochaton-Piallat ML (2002) Heterogeneity of smooth muscle cell populations cultured from pig coronary artery. *Arteriosclerosis, Thrombosis, and Vascular Biology* **22**, 1093–1099.

53 Gittenberger-De Groot AC, Deruiter MC, Bergwerff M & Poelmann RE (1999) *Smooth Muscle Cell Origin and Its Relation to Heterogeneity in Development and Disease*.

54 Iruela-Arispe M (2018) A dual origin for blood vessels. *Nature* **562**, 195–197.

55 Hennigs JK, Matuszcak C, Trepel M & Körbelin J (2021) Vascular endothelial cells: Heterogeneity and targeting approaches. *Cells* **10**.

56 Turgeon PJ, Chan GC, Chen L, Jamal AN, Yan MS, Ho JJD, Yuan L, Ibeh N, Ku KH, Cybulsky MI, Aird WC & Marsden PA (2020) Epigenetic Heterogeneity and Mitotic Heritability Prime Endothelial Cell Gene Induction. *The Journal of Immunology* **204**, 1173–1187.

57 Kojima I, Mogami H, Norio KN, Horoshi YH & Shibata H (1993) Modulation of Growth of Vascular Smooth Muscle Cells by Activin A. *Experimental Cell Research* **206**, 152–156.

58 Frank DB, Abtahi A, Yamaguchi DJ, Manning S, Shyr Y, Pozzi A, Baldwin HS, Johnson JE & de Caestecker MP (2005) Bone morphogenetic protein 4 promotes pulmonary vascular remodeling in hypoxic pulmonary hypertension. *Circulation Research* **97**, 496–504.

558 59 Pan CH, Chen CW, Sheu MJ & Wu CH (2012) Salvianolic acid B inhibits SDF-1α-stimulated cell
559 proliferation and migration of vascular smooth muscle cells by suppressing CXCR4 receptor.
560 *Vascular Pharmacology* **56**, 98–105.
561 60 Park SL, Won SY, Song JH, Kambe T, Nagao M, Kim WJ & Moon SK (2015) EPO gene
562 expression promotes proliferation, migration and invasion via the p38MAPK/AP-1/MMP-9
563 pathway by p21WAF1 expression in vascular smooth muscle cells. *Cellular Signalling* **27**, 470–
564 478.
565 61 Ghiselli G, Chen J, Kaou M, Hallak H & Rubin R (2003) Ethanol inhibits fibroblast growth factor-
566 induced proliferation of aortic smooth muscle cells. *Arteriosclerosis, Thrombosis, and Vascular*
567 *Biology* **23**, 1808–1813.
568 62 Yang N, Dong B, Song Y, Li Y, Kou L, Yang J & Qin Q (2020) Downregulation of miR-637
569 promotes vascular smooth muscle cell proliferation and migration via regulation of insulin-like
570 growth factor-2. *Cellular and Molecular Biology Letters* **25**.
571 63 Brizzi MF, Formato L, Dentelli P, Rosso A, Pavan M, Garbarino G, Pegoraro M, Camussi G &
572 Pegoraro L (2001) Interleukin-3 Stimulates Migration and Proliferation of Vascular Smooth
573 Muscle Cells A Potential Role in Atherogenesis. *Circulation* **103**, 549–545.
574 64 Li L, Blumenthal DK, Terry CM, He Y, Carlson ML & Cheung AK (2011) PDGF-induced
575 proliferation in human arterial and venous smooth muscle cells: Molecular basis for differential
576 effects of PDGF isoforms. *Journal of Cellular Biochemistry* **112**, 289–298.

577 65 Wang CH, Verma S, Hsieh IC, Hung A, Cheng TT, Wang SY, Liu YC, Stanford WL, Weisel RD, Li
578 RK & Cherng WJ (2007) Stem cell factor attenuates vascular smooth muscle apoptosis and
579 increases intimal hyperplasia after vascular injury. *Arteriosclerosis, Thrombosis, and Vascular*
580 *Biology* **27**, 540–547.
581 66 Li F, Duman-Scheel M, Yang D, Du W, Zhang J, Zhao C, Qin L & Xin S (2010) Sonic hedgehog
582 signaling induces vascular smooth muscle cell proliferation via induction of the G1 cyclin-
583 retinoblastoma axis. *Arteriosclerosis, Thrombosis, and Vascular Biology* **30**, 1787–1794.
584 67 Grosskreutz CL, Anand-Apte B, Dupláa C, Quinn TP, Terman BI, Zetter B & D'amore PA (1999)
585 Vascular Endothelial Growth Factor-Induced Migration of Vascular Smooth Muscle Cells in
586 Vitro. *Microvasc Res* **58**, 128–136.
587 68 Carthy JM, Luo Z & McManus BM (2012) WNT3A induces a contractile and secretory phenotype
588 in cultured vascular smooth muscle cells that is associated with increased gap junction
589 communication. *Laboratory Investigation* **92**, 246–255.
590 69 Kaneda H, Arao T, Matsumoto K, de Velasco MA, Tamura D, Aomatsu K, Kudo K, Sakai K, Nagai
591 T, Fujita Y, Tanaka K, Yanagihara K, Yamada Y, Okamoto I, Nakagawa K & Nishio K (2011)
592 Activin A inhibits vascular endothelial cell growth and suppresses tumour angiogenesis in gastric
593 cancer. *British Journal of Cancer* **105**, 1210–1217.
594 70 Zhang M, Qiu L, Zhang Y, Xu D, Zheng JC & Jiang L (2017) CXCL12 enhances angiogenesis
595 through CXCR7 activation in human umbilical vein endothelial cells. *Scientific Reports* **7**.

596 71 Carlini RG, Reyes AA & Romsmin M (1995) Recombinant human erythropoietin stimulates
597 angiogenesis in vitro. *Kidney International* **47**, 740–745.
598 72 Anagnostou A, Lee ES, Kessimian N, Levinsont R & Steiner M (1990) Erythropoietin has a
599 mitogenic and positive chemotactic effect on endothelial cells (hematopoietic growth factors).
600 *Proc Natd Acad Sci USA* **87**, 5978–5982.
601 73 Giraux J-L, Matoua S, Brosa A, Tapon-Bretaudierea J, Letourneur D & Fischer1 A-M (1998)
602 Modulation of human endothelial cell proliferation and migration by fucoidan and heparin.
603 *European Journal of Cell Biology* **77**, 352–359.
604 74 Brizzi MF, Garbarino G, Rossi PR, Pagliardi GL, Arduino C, Avanzi GC & Pegoraro L (1993)
605 Interleukin 3 stimulates proliferation and triggers endothelial-leukocyte adhesion molecule 1
606 gene activation of human endothelial cells. *J Clin Invest* **91**, 2887–2892.
607 75 Dallinga MG, Habani YI, Kayser RP, van Noorden CJF, Klaassen I & Schlingemann RO (2020)
608 IGF-binding proteins 3 and 4 are regulators of sprouting angiogenesis. *Molecular Biology*
609 *Reports* **47**, 2561–2572.
610 76 Battegay EJ, Rupp J, Iruela-Arispe L, Sage EH & Pech M (1994) PDGF-BB Modulates Endothelial
611 Proliferation and Angiogenesis In Vitro via PDGF B-Receptors. *The Journal of Cell Biology* **125**,
612 917–928.
613 77 Phillips GD & Stone AM (1994) *PDGF-BB induced chemotaxis is impaired in aged capillary*
614 *endothelial cells*.

615 78 Broudy VC, Kovach NL, Bennett LG, Lin N, Jacobsen FW & Kidd PG (1994) Human Umbilical
616 Vein Endothelial Cells Display High-Affinity c-kit Receptors and Produce a Soluble Form of the
617 c-kit Receptor. *Blood* **83**, 2145–2152.
618 79 Rivron NC, Raiss CC, Liu J, Nandakumar A, Sticht C, Gretz N, Truckenmüller R, Rouwkema J &
619 van Blitterswijk CA (2012) Sonic Hedgehog-activated engineered blood vessels enhance bone
620 tissue formation. *Proc Natl Acad Sci USA* **109**, 4413–4418.
621 80 Cross MJ & Claesson-Welsh L (2001) FGF and VEGF function in angiogenesis: signalling
622 pathways, biological responses and therapeutic inhibition. *TRENDS in Pharmacological Sciences*
623 **22**, 201–207.
624 81 Samarzija I, Sini P, Schlange T, MacDonald G & Hynes NE (2009) Wnt3a regulates proliferation
625 and migration of HUVEC via canonical and non-canonical Wnt signaling pathways. *Biochemical*
626 *and Biophysical Research Communications* **386**, 449–454.
627
628
629 **Figure Legends**
630
631 **Figure 1. bFGF broke the quiescence of SMCs, but not ECs**
632 At confluence, the mouse vascular smooth muscle cell line (MOVAS) and the mouse vascular
633 endothelial cell line (UV2) were treated with the indicated factor for three days in serum-free medium.
634 (A) Images of MOVAS and UV2 cells. The white arrow points to MOVAS cells with changed shape
635 after treatment with bFGF. The white asterisk denotes a cell-free area. The final concentration of each
636 factor is indicated in the bracket of each panel. Scale bars show 100 μm. Similar results were obtained
637 in three independent experiments. (B) Proportion of MOVAS cells with different shapes (flat

638 polygonal shape, and others including small spindle shape), and of UV2 cells (epithelial-like shape
639 and others) found in each group (n = 300 from three independent experiments). bFGF, basic fibroblast
640 growth factor; BMP4, bone morphogenetic protein 4; CXCL12, chemokine (C-X-C motif) ligand 12;
641 EPO, erythropoietin; FGFa, FGF acidic; IGF-II, insulin-like growth factor-II; IL-3, interleukin-3;
642 PDGF-BB, platelet-derived growth factor-bb; SCF, stem cell factor; SHH, sonic hedgehog; TGFβ1,
643 transforming growth factor beta 1; VEGF, vascular endothelial growth factor; WNT-3A, wingless-
644 type MMTV integration site family, member-3A.
645
646 **Figure 2. bFGF reduced cell size and increased proliferation in SMCs**
647 Confluent MOVAS and UV2 cells were treated with bFGF (20 ng/ml) or TGFβ1 (10 ng/ml) for three
648 days in serum-free medium. (A) Fluorescent images after staining with β-catenin (gray) and DAPI
649 (blue). Scale bars show 50 μm. Similar results were observed in three independent experiments. (B)
650 Cell size. Data are presented as the mean ± s.d. (n = 100 from three independent experiments). * $p <$
651 0.05 by Tukey's test. (C) Cell-free area per image. Data are presented as the mean ± s.d. (n = 9 from
652 three independent experiments). * $p < 0.05$ by Tukey's test. (D) Cell number per image. Data are
653 presented as the mean ± s.d. (n = 9 from three independent experiments). * $p < 0.05$ by Tukey's test.
654
655 **Figure 3. bFGF-induced SMC changes accompanied by reduced co-localization of TAGLN and**
656 **actin**
657 Confluent MOVAS or UV2 cells were treated with bFGF (20 ng/ml) or TGFβ1 (10 ng/ml) for three
658 days in serum-free medium. (A and C) Fluorescent images after staining with β-catenin (gray), actin
659 (green), and TAGLN (red). Scale bars show 20 μm. Similar results were observed in three
660 independent experiments. (B and D) Co-localization area of TAGLN and actin per image. Data are
661 presented as the mean ± s.d. (n = 9 from three independent experiments). * $p < 0.05$ by Tukey's test.
662
663 **Figure 4. bFGF decreased the expression of *Tagln* and *Srf* in SMCs, but not ECs**
664 (A) The expression of *Fgfr1* in B16, MOVAS, and UV2 cells was quantified using real-time PCR.
665 *B2m* was used for normalization. Data are presented as the mean ± s.d. (n = 5 from three independent

666 experiments). * $p < 0.05$ by Tukey's test. (B) Luciferase reporter assay of the *Tagln* promoter in
667 MOVAS and UV2 cells. The reporter activity was normalized to that of the co-transfected Renilla
668 luciferase plasmid. Data are presented as the mean ± s.d. (n = 5 per group). ** $p < 0.01$ versus
669 pGL4.15 vector control by the F-test, followed by Student's *t*-test. Similar results were obtained in
670 three independent experiments. (C) Confluent MOVAS and UV2 cells were treated with bFGF (20
671 ng/ml) or TGFβ1 (10 ng/ml) for three days in serum-free medium. The expression of *Tagln*, *Srf*, and
672 *Klf4* was quantified using real-time PCR. *B2m* or *Gapdh* was used for the normalization of *Tagln* and
673 *Klf4*, or *Srf*, expression. Data are presented as the mean ± s.d. (n = 5 from three independent
674 experiments). * $p < 0.05$ by Tukey's test.
675
676 **Figure 5. TGFβ1 failed to prevent bFGF-induced breakage of quiescence in SMCs**
677 At confluence, cells were treated with the indicated factor for three days in serum-free medium. (A)
678 Images of MOVAS and UV2 cells. White arrows point to MOVAS cells with changed shapes. White
679 asterisks denote cell-free areas. The final concentration of each factor is indicated in the bracket of
680 each panel. Scale bars show 100 μm. Similar results were obtained in three independent experiments.
681 (B) Proportion of MOVAS cells with different shapes (flat polygonal shape, and others including
682 small spindle shape), and of UV2 cells (epithelial-like shape and others) found in each group, (n = 300
683 from three independent experiments).

Figure 1

A

Vascular smooth muscle cell line (MOVAS) | **Vascular endothelial cell line (UV2)**

Control
ACTIVIN A (20 ng/ml)
BMP4 (100 ng/ml)
CXCL12 (20 ng/ml)
EPO (2 U/ml)
FGFa (10 ng/ml)
bFGF (20 ng/ml)
IGF-II (100 ng/ml)
IL-3 (20 ng/ml)
PDGF-BB (10 ng/ml)
SCF (100 ng/ml)
SHH (20 ng/ml)
TGFβ1 (10 ng/ml)
VEGF (20 ng/ml)
WNT-3A (20 ng/ml)

B

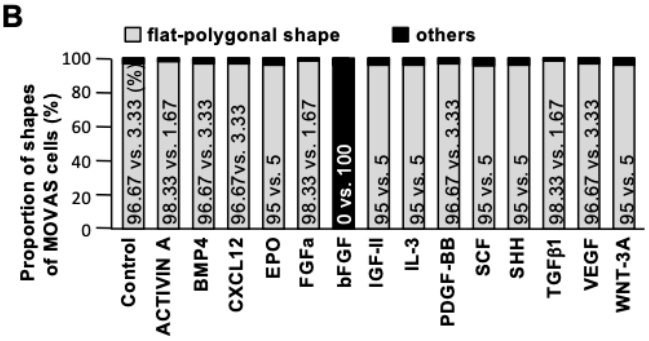

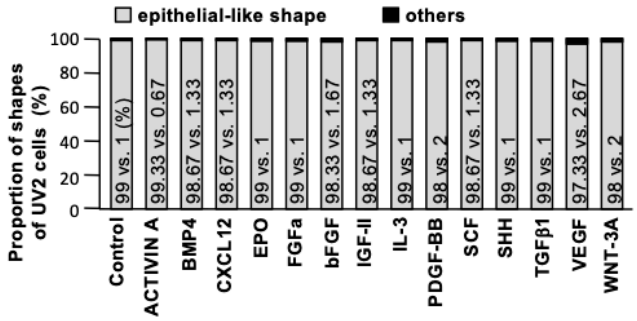

Figure 2

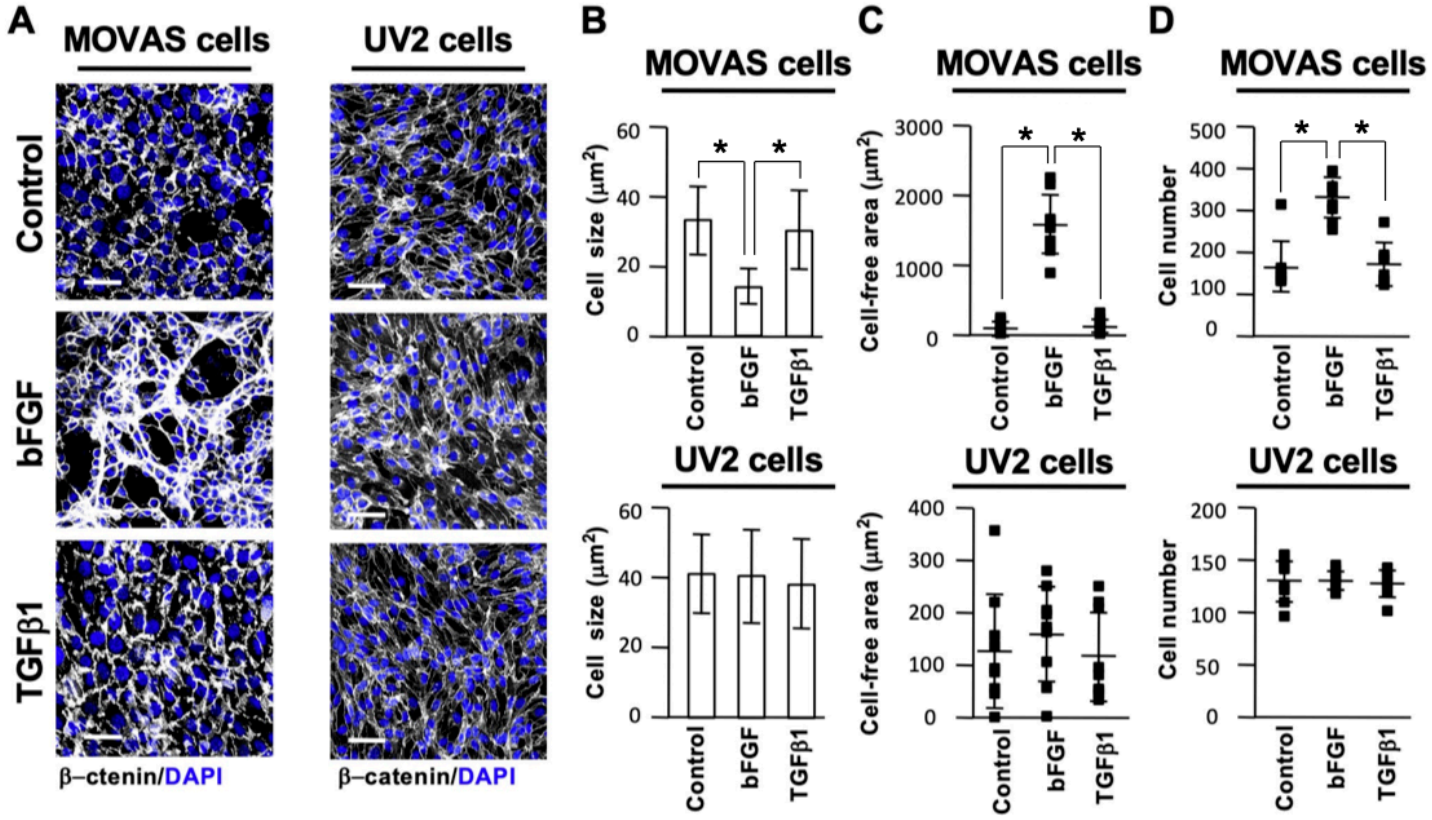
A
MOVAS cells
UV2 cells
Control
bFGF
TGFβ1
β–ctenin/DAPI
β–catenin/DAPI
B
MOVAS cells
Cell size (μm²)
60
40
20
0
*
*
Control
bFGF
TGFβ1
UV2 cells
Cell size (μm²)
C
MOVAS cells
Cell-free area (μm²)
3000
2000
1000
0
UV2 cells
Cell-free area (μm²)
400
300
200
100
0
D
MOVAS cells
Cell number
500
400
300
200
100
0
UV2 cells
Cell number
200
150
100
50
0

Figure 3

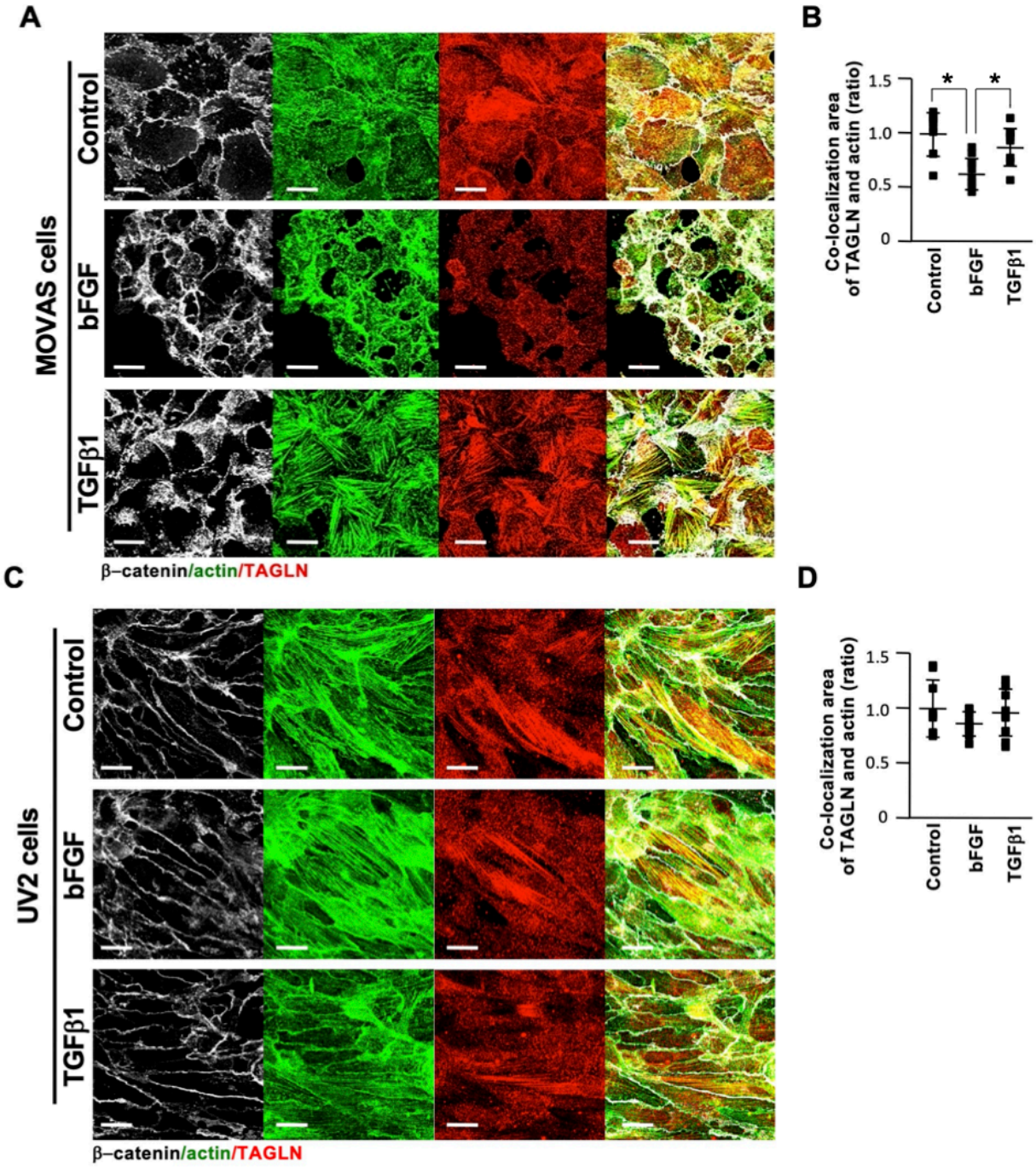
A
MOVAS cells
Control
bFGF
TGFβ1
β–catenin/actin/TAGLN
B
Co-localization area of TAGLN and actin (ratio)
1.5
1.0
0.5
0
*
*
Control
bFGF
TGFβ1
C
UV2 cells
Control
bFGF
TGFβ1
β–catenin/actin/TAGLN
D
Co-localization area of TAGLN and actin (ratio)
1.5
1.0
0.5
0
Control
bFGF
TGFβ1

Figure 4

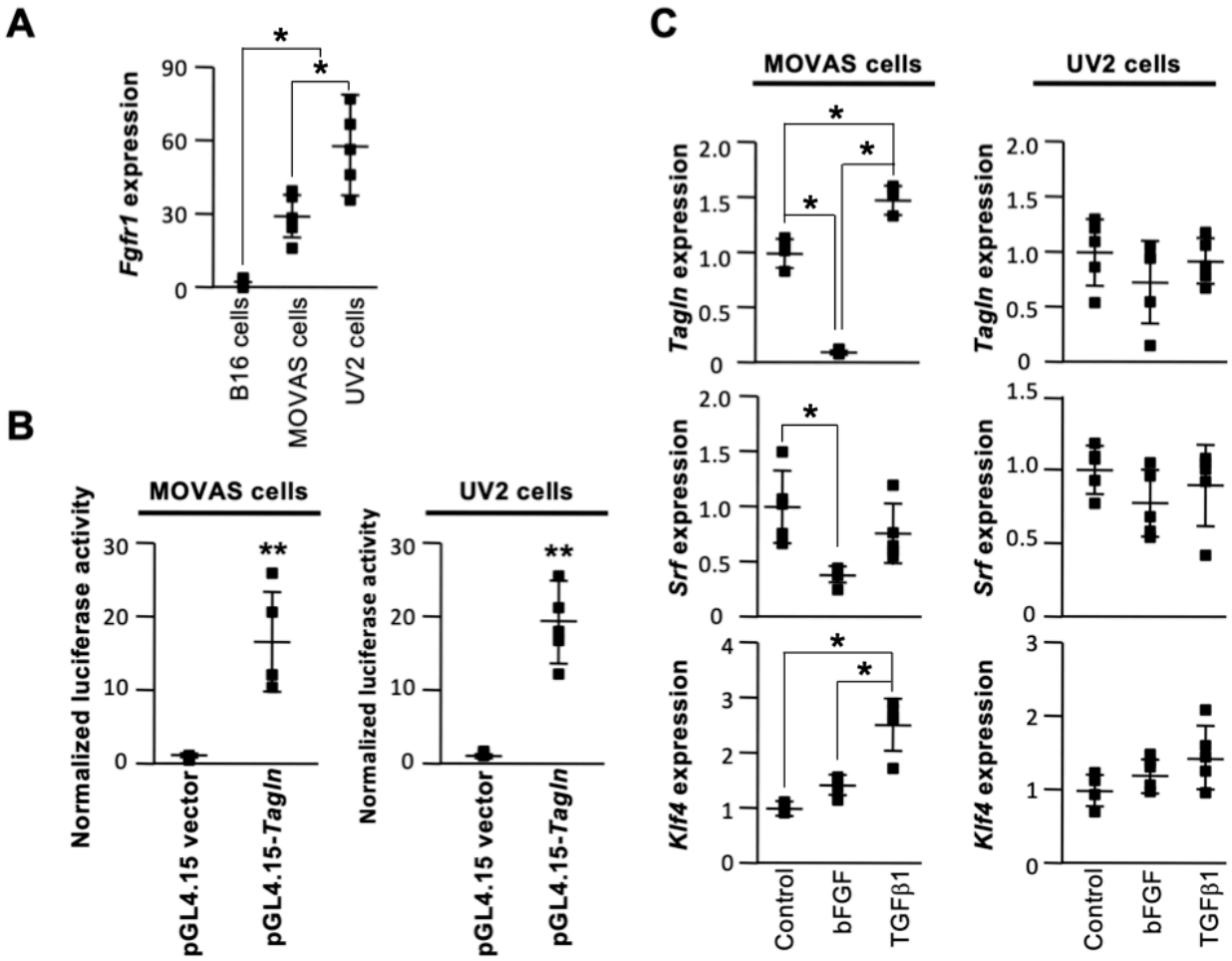
A
Fgfr1 expression
90
60
30
0
*
*
B16 cells
MOVAS cells
UV2 cells
B
MOVAS cells
UV2 cells
Normalized luciferase activity
30
20
10
0
**
pGL4.15 vector
pGL4.15-Tagln
C
MOVAS cells
UV2 cells
Tagln expression
Srf expression
Klf4 expression
Control
bFGF
TGFβ1

Figure 5

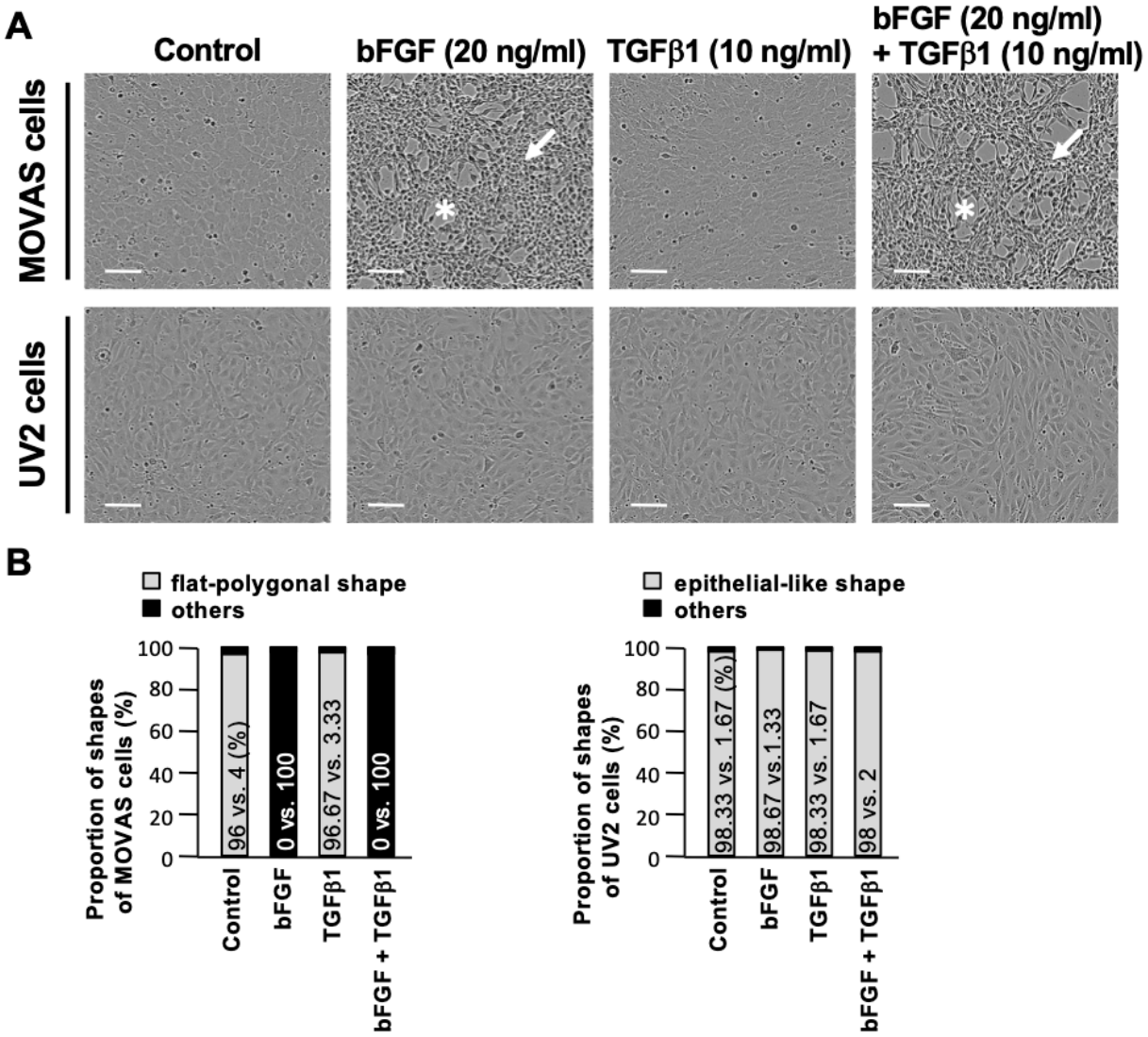
A
Control
bFGF (20 ng/ml)
TGFβ1 (10 ng/ml)
bFGF (20 ng/ml)
+ TGFβ1 (10 ng/ml)
MOVAS cells
UV2 cells
B
flat-polygonal shape
others
Proportion of shapes of MOVAS cells (%)
100
80
60
40
20
0
96 vs. 4 (%)
0 vs. 100
96.67 vs. 3.33
0 vs. 100
Control
bFGF
TGFβ1
bFGF + TGFβ1
epithelial-like shape
others
Proportion of shapes of UV2 cells (%)
98.33 vs. 1.67 (%)
98.67 vs.1.33
98.33 vs. 1.67
98 vs. 2

Supplementary Figures

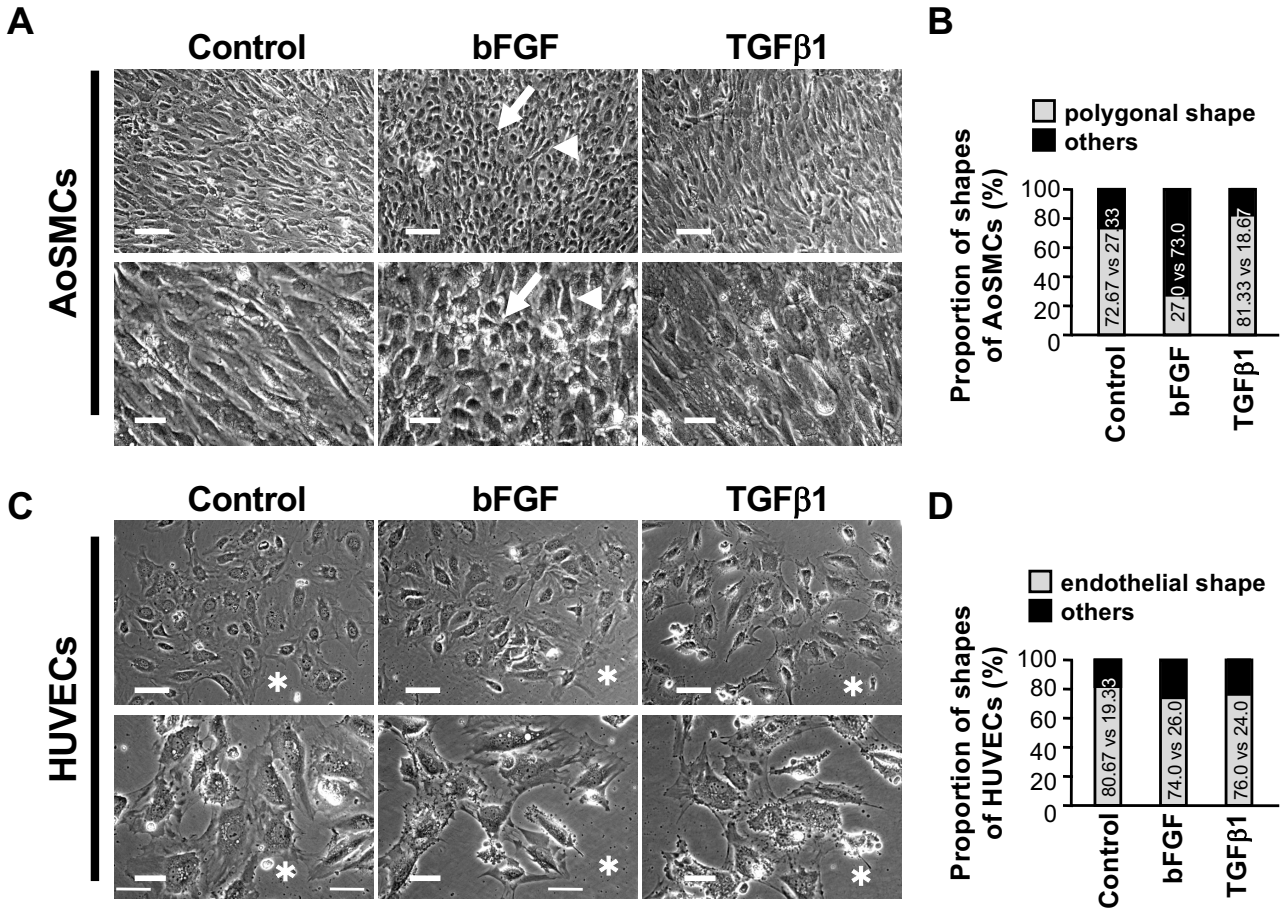

Fig. S1. bFGF broke the quiescence of human primary SMCs, but not human primary ECs
At confluence, human aortic smooth muscle cells (AoSMCs) and human umbilical vein endothelial cells (HUVECs) were treated with the bFGF (20 ng/ml) or TGFβ1 (10 ng/ml) for three days in 0.1% FBS medium (low serum medium). (A and C) Images of AoSMCs and HUVECs. White arrows point to AoSMCs with changed shape after treatment with bFGF, and white arrowheads point to polygonal shaped cells. The white asterisks denote cell-free spaces probably formed by the death of some HUVECs due to low serum stimulation. Scale bars show 90 μm (upper panels) and 40 μm (lower panels). Similar results were obtained in three independent experiments. (B and D) The proportion of AoSMCs with different shapes (polygonal shape, and others including small round shape), and of HUVECs (endothelial shape and others) found in each group (n = 300 from three independent experiments).

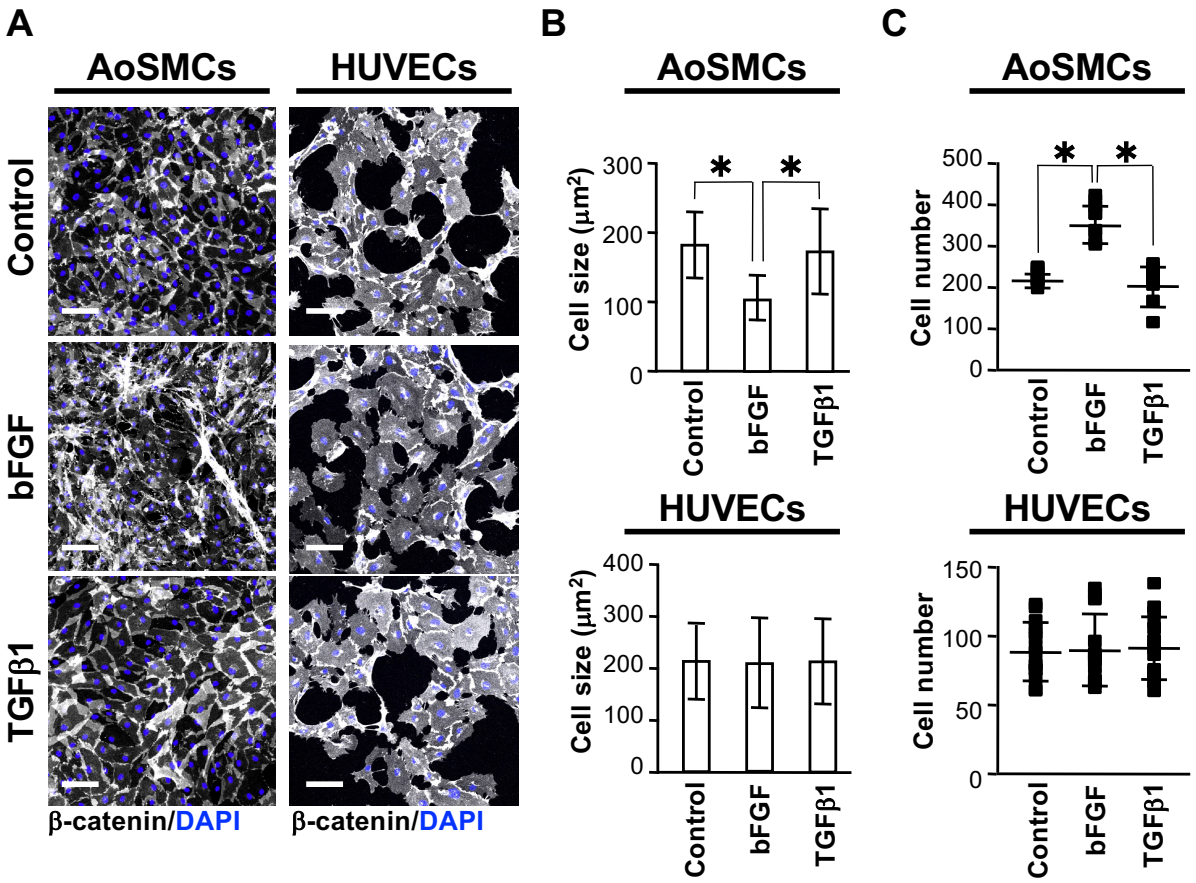

Fig. S2. bFGF reduced cell size and increased proliferation in primary SMCs
Confluent AoSMCs and HUVECs were treated with bFGF (20 ng/ml) or TGFβ1 (10 ng/ml) for three days in low serum medium. (A) Fluorescent images after staining with β-catenin (gray) and DAPI (blue). Scale bars show 100 μm. Similar results were observed in three independent experiments. (B) Cell size. Data are presented as the mean ± s.d. (n = 300 from three independent experiments). * $p < 0.05$ by Tukey's test. (C) Cell number per image. Data are presented as the mean ± s.d. [n = 9 (AoSMCs) or 15 (HUVECs) from three independent experiments]. * $p < 0.05$ by Tukey's test.

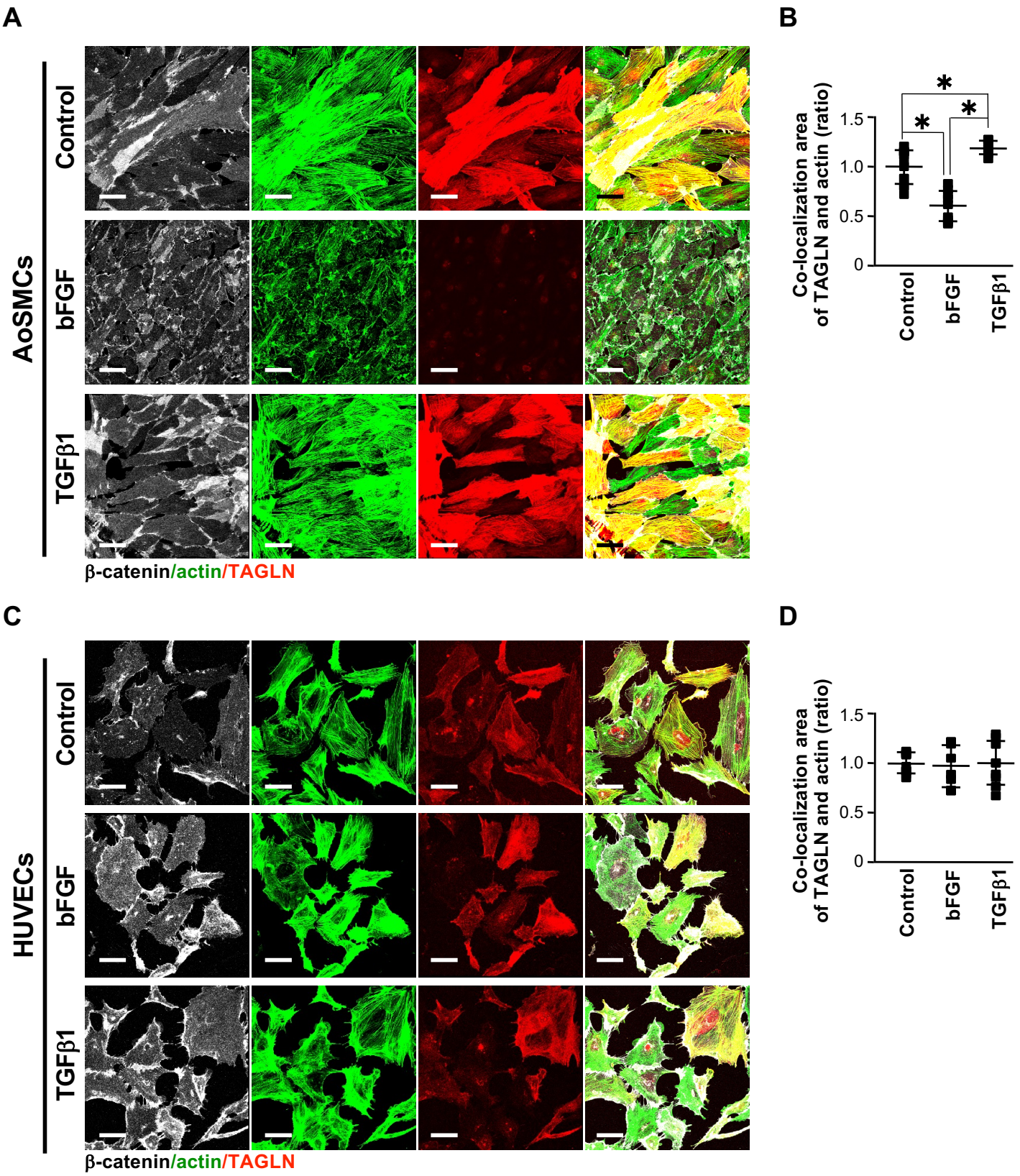

Fig. S3. bFGF-induced primary SMCs changes accompanied by reduced co-localization of TAGLN and actin

Confluent AoSMCs and HUVECs were treated with bFGF (20 ng/ml) or TGFβ1 (10 ng/ml) for three days in low serum medium. (A and C) Fluorescent images after staining with β-catenin (gray), actin (green), and TAGLN (red). Scale bars show 50 μm. Similar results were observed in three independent experiments. (B and D) Co-localization area of TAGLN and actin per image. Data are presented as the mean ± s.d. (n = 9 from three independent experiments). * $p < 0.05$ by Tukey's test.

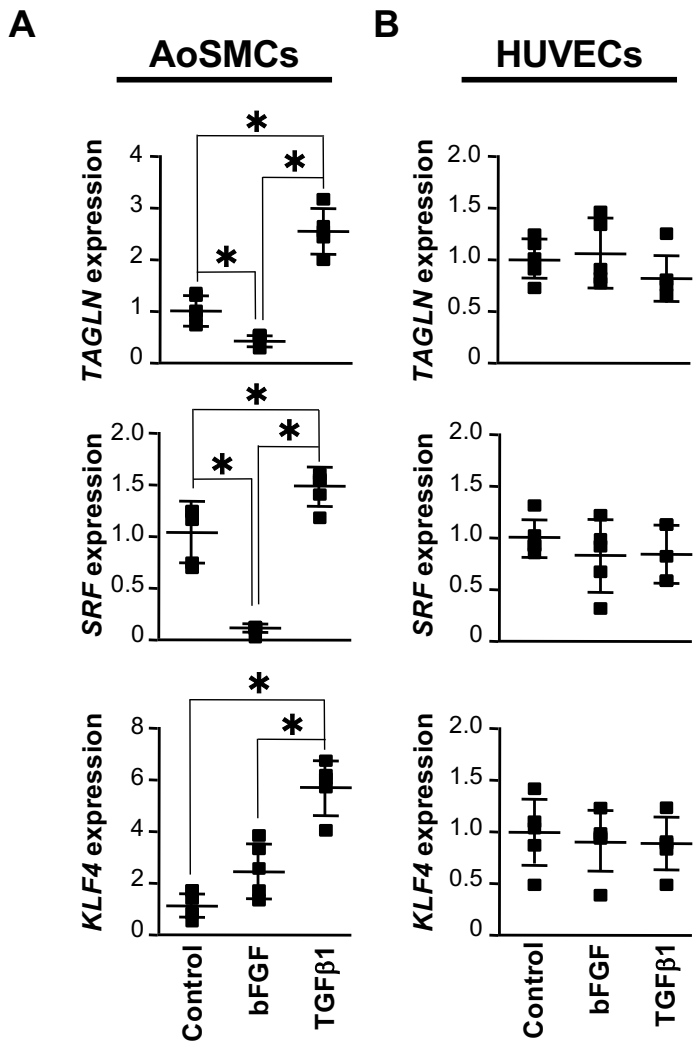

Fig. S4. bFGF decreased the expression of *TAGLN* and *SRF* in primary SMCs.
Confluent AoSMCs and HUVECs were treated with bFGF (20 ng/ml) or TGFβ1 (10 ng/ml) for three days in low serum medium. The expression of *TAGLN*, *SRF*, and *KLF4* was quantified using real-time PCR. *beta-ACTIN* was used for the normalization of gene expression. Data are presented as the mean ± s.d. (n = 5 from three independent experiments). * $p < 0.05$ by Tukey's test.

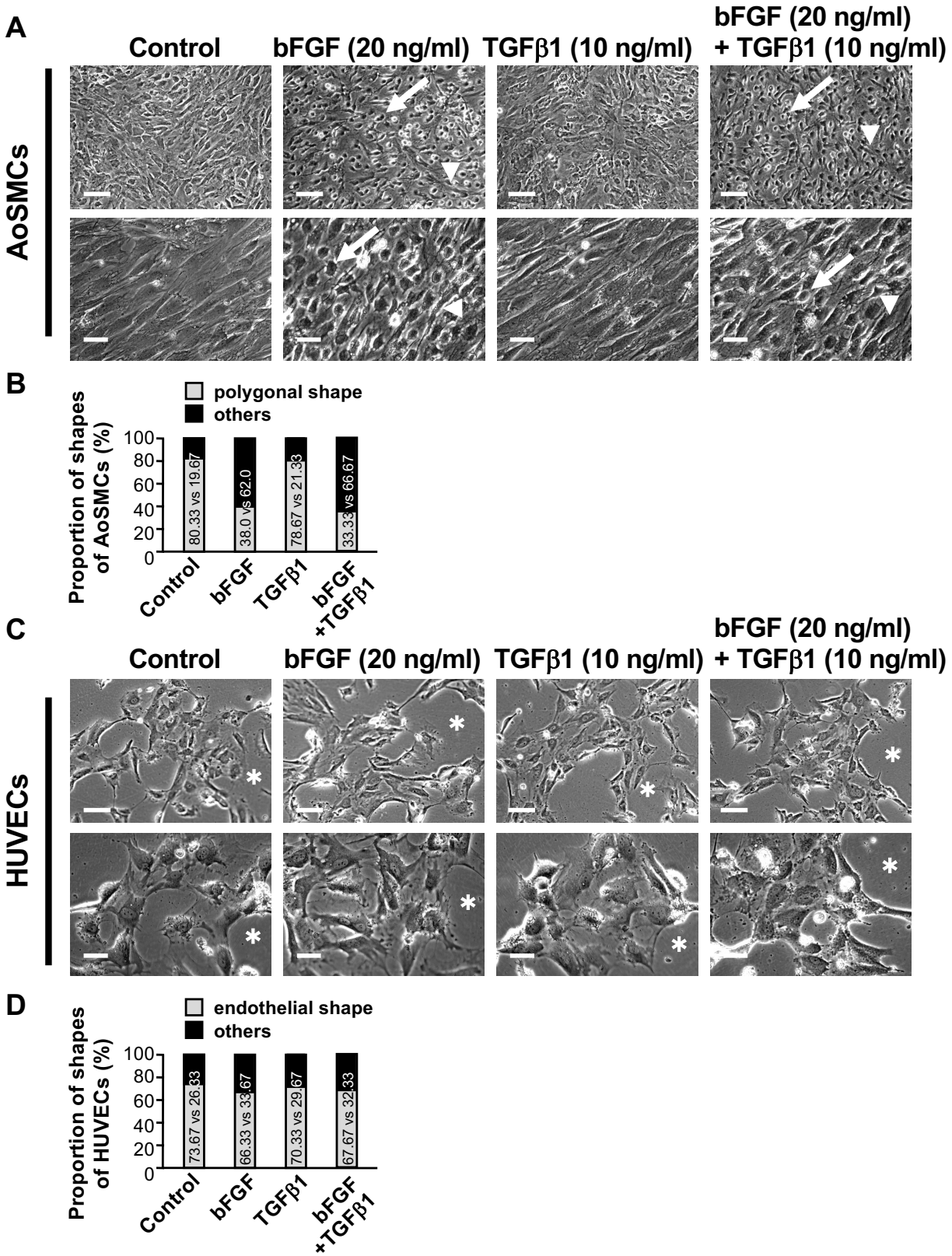

Fig. S5. TGFβ1 failed to prevent bFGF-induced breakage of quiescence in primary SMCs

At confluence, cells were treated with the indicated factor for three days in low serum medium. (A and C) Images of AoSMCs and HUVECs. White arrows point to AoSMCs with changed shape after treatment with bFGF without or with TGFβ1, and white arrowheads point to polygonal shaped cells. The white asterisks denote cell-free spaces probably formed by the death of some HUVECs due to low serum stimulation. The final concentration of each factor is indicated in the bracket of each panel. Scale bars show 90 μm (upper panels) and 40 μm (lower panels). Similar results were obtained in three independent experiments. (B and D) The proportion of AoSMCs with different shapes (polygonal shape, and others including small round shape), and of HUVECs (endothelial shape and others) found in each group (n = 300 from three independent experiments).

Graphical Abstract

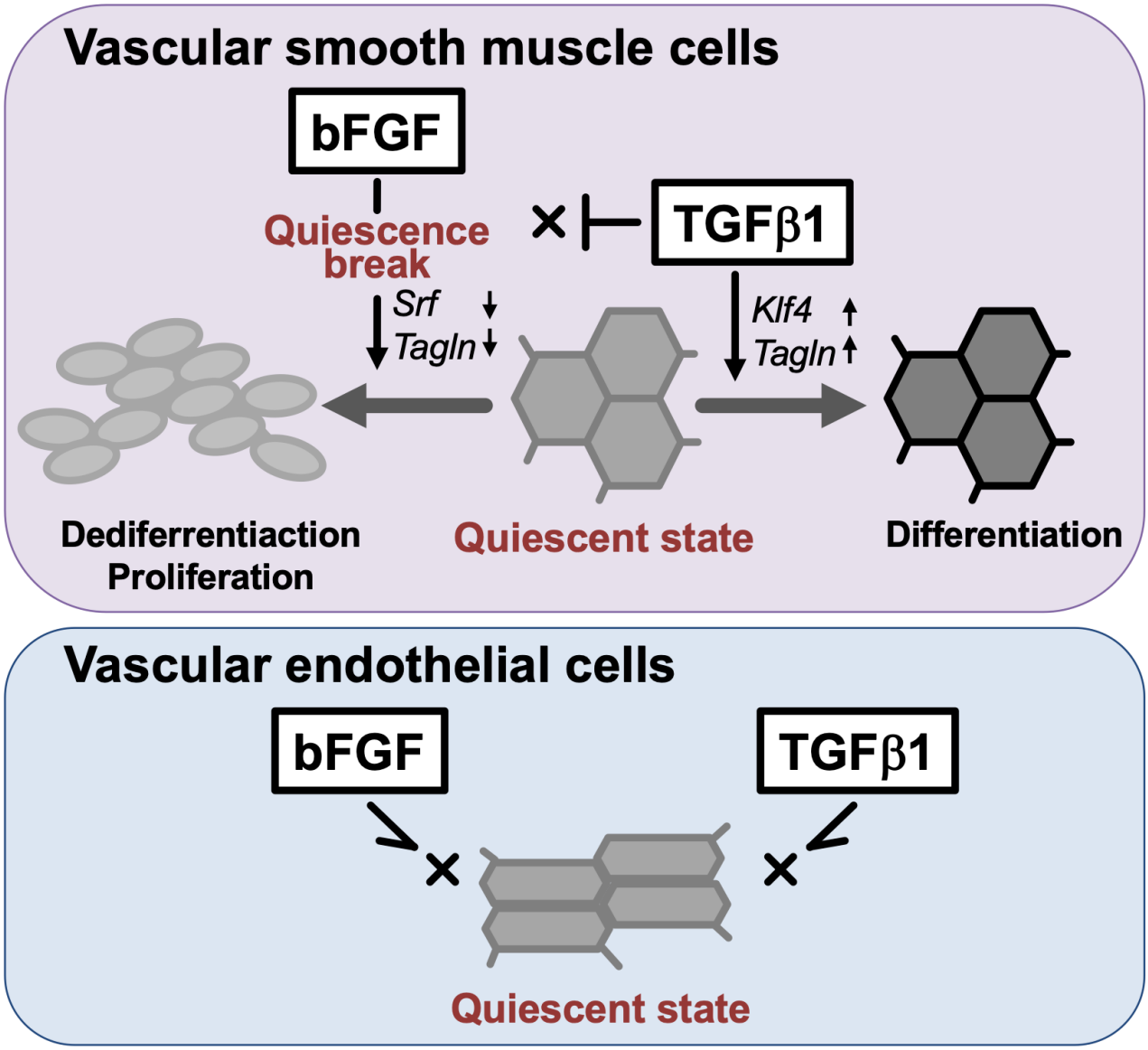

bFGF induced breakage of quiescence in vascular smooth muscle cells, and led to dedifferentiation and proliferation accompanied by reduced expression of a transcription factor *Srf* and a myogenic marker *Tagln*. TGFβ1 upregulated a transcription factor *Klf4* and *Tagln* expression and induced differentiation; however, it failed to inhibit bFGF-induced quiescence breakage. bFGF and TGFβ1 didn't affect the quiescent vascular endothelial cells.